Felix *et al. Geoscience Letters* (2025) 12:49
https://doi.org/10.1186/s40562-025-00422-5

Geoscience Letters

RESEARCH LETTER

Open Access

Funwave-based open-access mapping applications (FUNMAP) applied to Tsunami modelling from the Manila Trench to Manila Bay, Philippines

Raquel Felix[1,2*], Elaine Hui Zhi Tan[2,3], Masashi Watanabe[4], Andrea Verolino[2], Jun Yu Puah[2,3] and Adam Switzer[2,3]

Abstract

Developing user-friendly applications bridges the gap between models and target users, aiding in more efficient learning and optimizing workflow. In this study, we contribute to bridging this gap in the tsunami modelling community by developing two offline, free standalone applications: the Input and Output FUNMAP apps. These tools are built on the open-source Fully Nonlinear Boussinesq Wave Model - Total Variation Diminishing version (FUNWAVE-TVD), a well-established and extensively validated model. The Input app assists in setting up simulation input files and running the FUNWAVE executable, while issuing visual warnings to help prevent errors. The Output app processes simulation results to generate wave height and current maps, as well as virtual gauge plots, with export options compatible with GIS and vector editing platforms. We tested the apps using sample cases from FUNWAVE-TVD and applied them to simulate tsunami hazards in Manila Bay, Philippines, under a hypothetical Mw 8.8 earthquake scenario along the southern Manila Trench. The results show that the presence of the submarine canyon at the bay entrance, along with the complex coastlines of Luzon, Lubang, and Mindoro Islands, influences the arrival of multiple waves in Manila Bay. The highest waves were observed at the bay entrance headlands and southern coasts, with high current velocities expected along the entire coastline. This case study demonstrates the effectiveness of the FUNMAP apps in generating tsunami simulation maps and plots.

Keywords Standalone Tsunami modelling apps, FUNWAVE apps, FUNMAP, Tsunami model apps, Manila Bay tsunami, Manila Trench tsunami

*Correspondence:
Raquel Felix
rf761@bath.ac.uk
[1] Present Address: Department of Architecture and Civil Engineering, University of Bath, Bath BA2 7AY, United Kingdom
[2] Earth Observatory of Singapore, Nanyang Technological University, 50 Nanyang Ave, Singapore 639798, Singapore
[3] Asian School of the Environment, Nanyang Technological University, 50 Nanyang Ave, 639798 Singapore, Singapore
[4] School of Ocean and Earth Science, University of Southampton, Southampton SO14 3ZH, United Kingdom

Introduction

Open access to models and applications can attract a broader range of users, and a user-friendly interface further enhances accessibility and adoption. In the tsunami modelling field, several modelling tools and web applications with user-friendly graphical user interfaces have been developed. These include online platforms such as ComMIT by NOAA (Merati et al 2010), iCOMCOT by Lin et al (2015), and Delft Dashboard (Van Ormondt et al 2020). The Community Model Interface for Tsunami (ComMIT) is based on the Method of Splitting Tsunami (MOST) model. iCOMCOT utilizes a modified version of the Cornell Multigrid Coupled Tsunami Model (Lin and

Liu 1998; Wang et al 2011), while Delft Dashboard supports Delft3D (Lesser et al 2004), XBeach (Roelvink et al 2009, 2018), and WAVEWATCH III (Tolman et al 2009). All of these models (COMCOT, MOST, and Delft3D) can simulate tsunami propagation based on non-linear shallow water equations. To our knowledge, no open-source platform currently exists for tsunami models that has an option to use Boussinesq equations, particularly one that can be downloaded and used offline.

Here, we introduce two user-friendly, offline desktop applications based on the FUNWAVE-TVD model-a fully nonlinear Boussinesq wave model with Total Variation Diminishing (TVD) capabilities. FUNWAVE is a phase-resolving, time-stepping Boussinesq model initially developed by Kirby et al (1998), building on the work of Wei et al (1995). The Boussinesq model (nonlinear dispersive wave model) can consider the dispersion effects during tsunami propagation and simulate the bores or soliton fissions (Watanabe et al 2022). In the case of solitary waves over the uniform sloping beach, the Boussinesq model gives a better representation of the wave evolution before the breaking point than the nonlinear shallow water equation (Liang et al 2013). The FUNWAVE-TVD is the Total Variation Diminishing (TVD) version of FUNWAVE developed by (Shi et al 2012) and it was developed based on a complete set of fully nonlinear Boussinesq equations with vertical vorticity correction (Shi et al 2012). In FUNWAVE-TVD, the generation of sea surface displacement can be initiated by importing pre-configured files, using a wavemaker, simulating meteotsunamis, modelling vessel conditions, and including the effects of sediment transport.

The aim of this paper is to make learning and using the FUNWAVE model more accessible, especially for those new to tsunami modelling. By simplifying the process through the development of applications with graphical user interfaces, users can focus more on the analytical aspects of their research. We demonstrate the functionality of the two applications we have developed by assessing tsunami hazards in Manila Bay, Philippines, in response to a potential rupture of the southern segment of the Manila Trench.

Standalone applications

We selected the FUNWAVE-TVD model, specifically the version 4.6, as the basis for our applications due to its publicly available code and examples on GitHub, as well as support from an active online user community. We named our applications "FUNMAP" to clearly associate them with the FUNWAVE model and highlight their roles in modelling tsunamis and creating maps (Figs. 1 and 2). We developed the apps using MATLAB App Designer and packaged them with the Application Compiler, producing versions compatible with both Windows and macOS. Although the apps were developed using a licensed version of MATLAB, they do not require MATLAB to run. The apps can be executed using the free MATLAB Runtime, which is included in the installation packages we provide. For users with access to MATLAB, an alternative installer is available that integrates the

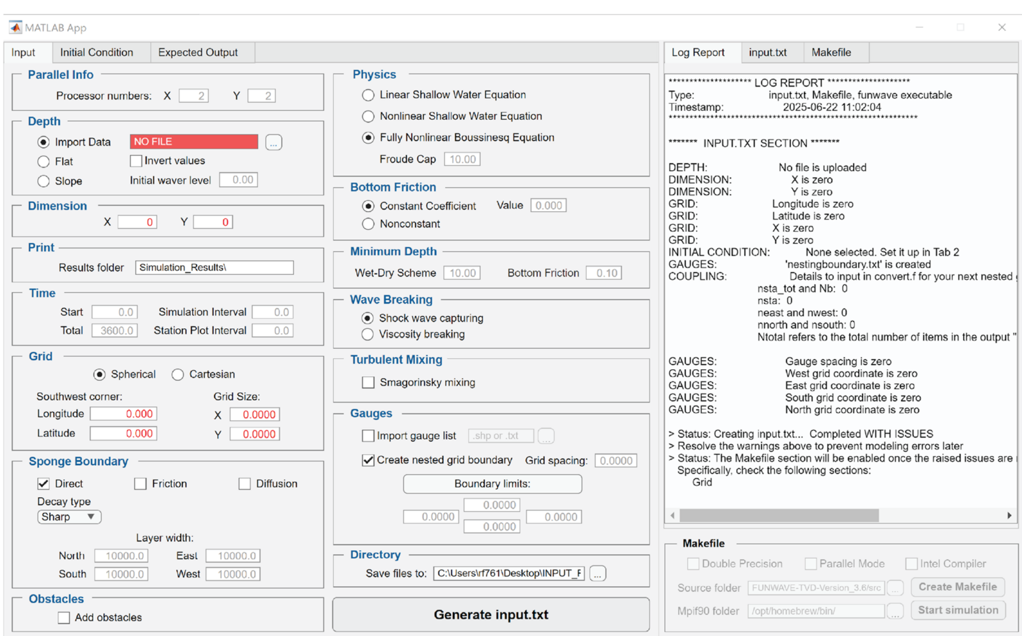

Fig. 1 The interface of the Input FUNMAP app. The enlarged version of this is shown in Supplementary Figure S1

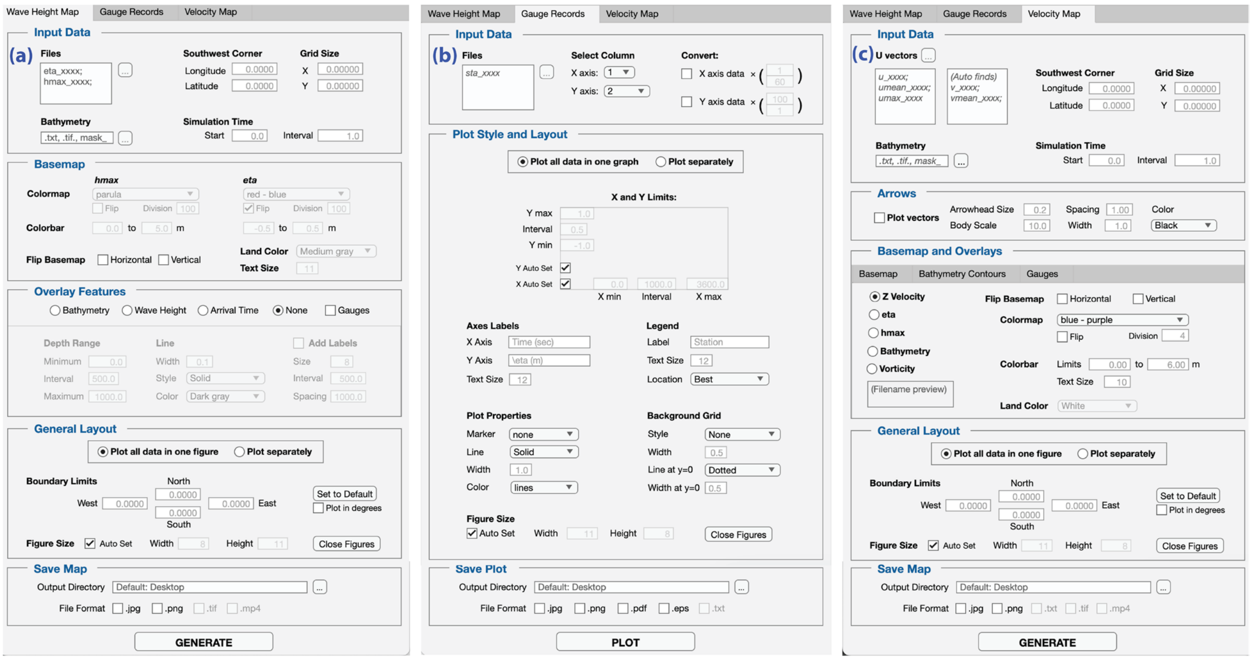

Fig. 2 The interface of the Output FUNMAP app, used for processing the output files generated from the tsunami simulation. Shown are the interfaces of the (**a**) Wave Height Map tab, (**b**) Gauge Record tab, and (**c**) Velocity Map tab. The enlarged versions of each panel are shown in Supplementary Figures S2 to S4

FUNMAP apps as in-app features within the software. A brief overview of each app is presented in the following subsections, with more detailed descriptions available in the user manual.

Input FUNMAP app

This app is for preparing the necessary files for tsunami simulations (Fig. 1). It also includes an option to create and run the executable program directly on the local desktop. The interface of the app is organised into three columns: the first two columns are dedicated to setting up input parameters and feature three tabs - 'Input', 'Initial Condition', and 'Expected Output'. The third column displays previews of the generated files: log report, input.txt, and Makefile.

The 'Input' tab configures the main parameters, while the 'Initial Condition' tab sets up tsunami initiation, with options including imported U-V-Z files, internal wavemaker, meteotsunami/landslide, or vessel. An additional option allows for including sediment effects. The 'Expected Output' tab provides a checklist of outputs the user want the model to generate.

To enhance accessibility, default values are preset in the text boxes, and tooltips are provided for additional context. When generating the input.txt file, the app checks for missing files or values, as well as unchanged non-zero defaults that may lead to errors, and lists them in the log report. In the app interface, such issues are highlighted by changing the font colour to red. Minor issues are automatically resolved-for example, swapping colourbar limits when necessary-and these adjustments are also recorded in the log report.

Output FUNMAP app

This app is designed to generate figures and animations from the output files of tsunami simulations. It consists of three main tabs, each functioning independently (Fig. 2). The first tab creates wave height maps, the second plots virtual gauge records, and the third generates velocity maps. Output maps can be saved as raster files (.jpg,.png), georeferenced raster files (.tif), or animation files (.mp4). Gauge plots can be exported as raster files (.jpg,.png), vector files (.pdf,.eps), or as text files containing gauge records and raw velocity data.

We tested the functionality of the FUNMAP apps using selected sample cases from FUNWAVE version 4.6. A side-by-side comparison between the maps generated by the app and the sample maps included in FUNWAVE is presented in the final section of the FUNMAP User Manual. Additionally, we evaluated the usability of the FUNMAP apps through a case study conducted in Manila Bay, Philippines.

Tsunami modelling: the Manila Bay case study

The aim of our case study is to model tsunami propagation toward Manila Bay, Philippines, generated by a hypothetical Mw 8.8 rupture of the southern segment of the Manila Trench, and to provide an initial tsunami hazard assessment. Manila Bay is selected as the study area because, to date, no focused tsunami hazard assessments have been conducted for this region in relation to a rupture along the Manila Trench (i.e., originating from an earthquake source). Previous studies have primarily focused on neighbouring countries and coastlines facing the South China Sea (e.g., Wu 2012; Nguyen et al 2014; Sun and Niu 2025). A previous tsunami hazard assessment has been conducted for the South China Sea, with Manila Bay included as one of the study areas; however, the study considered potential volcanic meteotsunamis as the source (Verolino et al 2025b). Assessing tsunami hazard in Manila Bay is particularly important due to its densely populated coastline (WorldPop 2024), primarily because the capital city is located in this area and because the Port of Manila-the largest and busiest in the Philippines-is situated here (Fig. 3).

Manila Bay morphology

Manila Bay, situated on the west coast of Luzon Island in the Philippines, opens into the South China Sea (Fig. 3). Its ~20-km-wide entrance is divided into two channels by Corregidor Island. The bay slopes southwest at an angle of 3° toward its mouth, reaching a maximum depth of 80 m. Beyond the entrance lies a submarine canyon striking nearly east–west (strike length: ~60 km, maximum width: ~30 km), with its shallow tip oriented toward the bay's mouth. The presence of the canyon causes the water depth to drop to ~1.5 km within a short distance from the coast. South of the canyon is the shallow Verde Island Passage, bordered by Luzon Island, Lubang Island, and Mindoro Island. These morphological descriptions are based on 50-m resolution bathymetry, interpolated and analysed using the most recent dataset from the National Mapping and Resource Information Authority (NAMRIA) of the Philippines.

Manila trench tectonics

The nearest tsunamigenic source to Manila Bay is the north–south striking, 10 – 50°E-dipping Manila Trench. It is formed by the convergence of the Philippine Sea

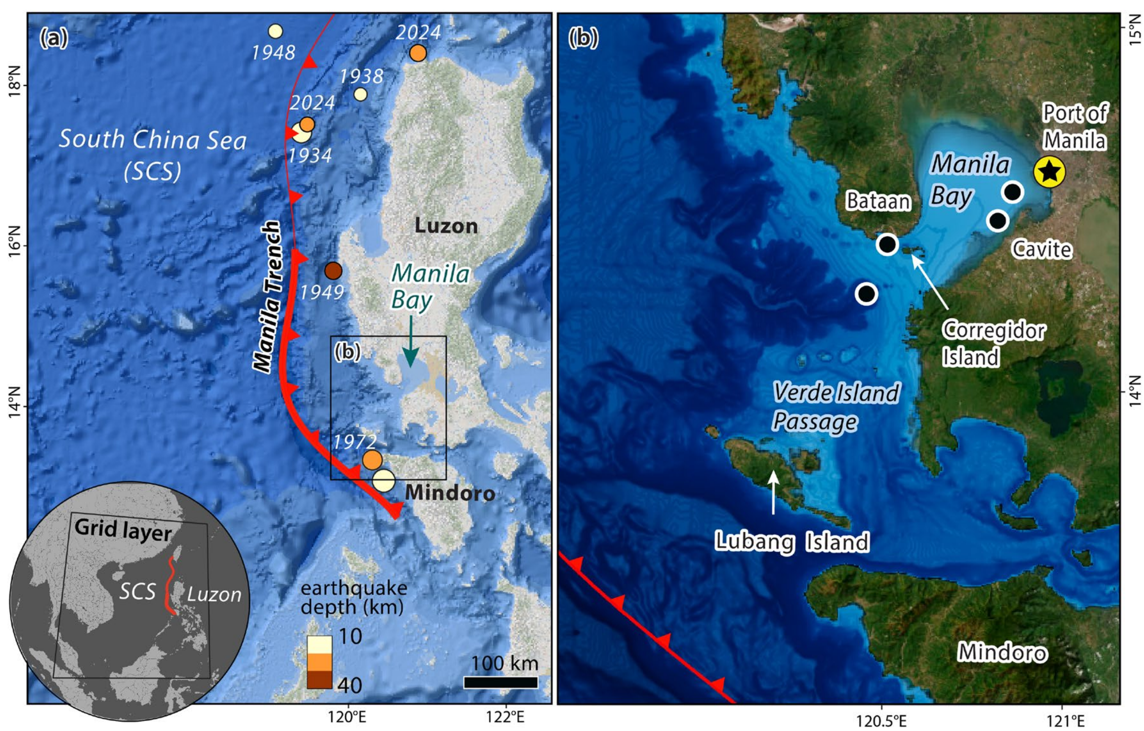

Fig. 3 (**a**) Location map of Manila Bay. The extent of the grid layer used in the modelling is shown on the inset map. The thicker line on the Manila Trench marks the extent of the tsunami source for this study. Circles - Mw 7.0 to 7.6 earthquakes between 1900 and 2006 (source: USGS 2024). The December 2024 Mw 5.0 and 5.7 earthquakes are also included in the map (source: PHIVOLCS 2024). The labels indicating the exact magnitude and date of occurrence for each event are shown in Supplementary Figure S5. (**b**) Close-up view of the complex coastline and bathymetry in the study area. A submarine canyon points towards Manila Bay. DotS - virtual gauge stations. Star - location of Manila, the capital city. The basemaps for (**a**) and (**b**) are ESRI maps available for use in QGIS

Plate and the Eurasian Plate, where the South China Sea is being subducted (Armada et al 2020). The Manila Trench has a slip rate between 50–90 mm/year and a coupling ratio of 0.4 (Bautista et al 2001; Hsu et al 2012, 2016). Since the 1560s, no earthquakes with moment magnitudes exceeding Mw 7.8 have been recorded along the Manila Trench (Megawati et al 2009; USGS 2024). However, historical and seismic records indicate that it generated earthquakes with magnitudes ranging from Mw 7.0 to 7.6 between 1900 and 2006. Although of lower magnitudes, it is noteworthy that the Manila Trench generated two earthquake clusters in December 2024 (ranging from Mw 4.6 to 5.7), attributed to different segments of the trench due to differences in their faulting mechanisms (PHIVOLCS 2024). Although these records suggest that the Manila trench has not generated larger than Mw 7.8 earthquakes, past geodetic and tsunamigenic studies suggested the possibility of earthquakes occurrence exceeding Mw 9.0 (Megawati et al 2009; Wu and Huang 2009; Nguyen et al 2014; Qiu et al 2019). This potential is further supported by the convergence of historical and sedimentological evidence (Yu et al 2009; Ramos et al 2012; Sun et al 2013; Lu et al 2019). However, it is important to acknowledge that distinguishing between storm and tsunami deposits remains a significant challenge at this stage.

Tsunami modelling setup

Early studies of tsunami hazards due to the Manila Trench assumed a full-length rupture of the fault (e.g., Megawati et al 2009; Wu and Huang 2009; Nguyen et al 2014). However, more recent studies suggest that piecewise rupture is more likely due to variations in fault properties and the presence of bathymetric asperities (Hsu et al 2012; Li et al 2016). Consequently, Li et al (2016) and Qiu et al (2019) proposed dividing the fault into three segments to more accurately represent its structural characteristics. In this study, we focused on the possibility of a rupture in the southern segment of the Manila Trench, as this segment is closest to our study site at Manila Bay.

Based on the rupture area of the southern segment, it can generate a maximum earthquake magnitude of Mw 8.8, as calculated using the earthquake scaling laws of Papazachos et al (2004) and Blaser et al (2010). Using the seismic moment formula (Keiiti 1966), we calculated an average slip of 10.3 m. To determine the heterogenous slip distribution across the fault plane of the southern Manila Trench segment, we adopted the configuration corresponding to the worst-case scenario for a Mw 8.8 event in Manila Bay, as identified in the probabilistic tsunami hazard assessment for Southeast Asian countries bordering the South China Sea by Tan et al (2023). The slip distributions in that study are generated using the RupGen model developed by Mai and Beroza (2000, 2002). These parameters, along with the fault properties of the Manila Trench defined by Hsu et al (2012), were used as inputs to generate the surface deformation using Okada (1985) model that assumes elastic half-space deformation. The computed seafloor deformation is assumed to be instantaneously and vertically transferred to the sea surface, and is therefore used as the initial condition (i.e., the tsunami at t = 0) in our tsunami simulations.

The FUNWAVE-TVD model is used for the tsunami modelling. The primary input file required to initiate the model is prepared using the Input FUNMAP application. Bathymetric data are provided at a 500 m resolution, interpolated from the 2024 GEBCO grid (GEBCO Compilation Group 2024) and supplemented with water depth points from NAMRIA, Philippines. The NAMRIA data were incorporated to enhance the quality of the interpolation, particularly in shallow regions where GEBCO data points are sparse within the study area. Although we initially created a 50-meter resolution bathymetric grid to capture the detailed morphology of Manila Bay, we opted to use a resampled grid with a 500-meter resolution for this study. This decision was made because we are using only a single numerical grid layer for our simulation, as this work serves as a preliminary assessment of tsunami hazards in Manila Bay. The 500-meter resolution is sufficient to capture large-scale features that could significantly influence tsunami behaviour in the region-specifically, the submarine canyon, as well as the shape and orientation of Luzon, Lubang and Mindoro Islands (Fig. 3a).

Although FUNWAVE-TVD is primarily a Boussinesq-type model, we used its linear shallow water equation function in our modelling. This is because the water depth within Manila Bay (≤80 m) is considerably smaller than the extent of the earthquake rupture area (∼ 500 km × 150 km), making dispersion effects negligible. To quantify the relevance of dispersion effects in our tsunami model, we applied the dispersion time (τ) formula introduced by Glimsdal et al (2013), which is defined as:

$$\tau = \frac{4h_0^2 L}{\lambda^3}$$

where h_0 is the water depth at the source, L is the distance from the source to the shoreline, and λ is the width of the tsunami source. Dispersion effects are considered negligible when $\tau < 0.01$. In the case of Manila Bay, the average depth at the source is approximately 2.5 km, the estimated source width is ∼150 km, and the distance to the shoreline, specifically to the Port of Manila, is ∼ 55 km. Substituting these values into the formula yields

$\tau \approx 0.00041$, indicating that dispersion effects in our study are negligible. This aligns with the conclusion of Glimsdal et al (2013) stating that dispersion is not needed for tsunami propagation in the near-field when dealing with large earthquake scenarios. Hence, the use of the linear shallow water equation is sufficient for this study.

We did not select a wave model to use in this study solely based on its primary governing equations. Instead, FUNWAVE-TVD was chosen due to its open-source availability and comprehensive documentation which are both important factors in our aim to develop a user-friendly application based on pre-existing models. We initially considered using its Boussinesq capabilities, however, our preliminary analysis confirmed that for the Manila Bay scenario, characterised by a near-field tsunami source and shallow water depths, the use of the linear shallow water equations is more appropriate. The primary goal in this study is to identify which areas within the bay are most likely to be impacted by tsunami waves, rather than to resolve fine-scale wave dynamics or inundation behaviour. If the study aimed to capture detailed wave height variations near the coast or perform inundation modelling, then the use of nonlinear shallow water equations or Boussinesq-type models would be more appropriate for this study.

The numerical grid we used covers the entire South China Sea. This broad domain helps minimize the influence of wave reflections at the boundaries on the tsunami results within Manila Bay. Additionally, a 100 km-thick sponge layer was implemented at the grid boundaries to absorb outgoing waves and reduce artificial reflections (Fig. 3a).

A spherical grid was applied, with a spatial resolution of 0.0045 arc degrees. We employed a second-order spatial discretization scheme. The default values for the Courant-Friedrichs-Lewy (CFL) number and the Froude cap—0.5 and 0.3, respectively - are used. The total simulation time was set to 14 h to ensure that all relevant tsunami waves entering Manila Bay were captured.

To gain a general understanding of the tsunami waveforms entering Manila Bay, we placed a virtual gauge station at the shallowing tip of the submarine canyon, at a depth of 100 m (Fig. 3b). This location was selected because the shallowing portion of the canyon is where tsunami waves are expected to arrive first, as demonstrated in studies by Iglesias et al (2014) and Linthon and Koshimura (2019) on the influence of submarine canyons on coastal wave propagation. We also added three gauges at a water depth of 20 m near the coastline of Port of Manila, and in the populated areas of Cavite and Bataan provinces (Fig. 3b). The placement of the gauges was also based on our preliminary simulation results, which indicate that these points (i.e., the gauge locations) lie along coastlines expected to experience the highest tsunami heights. The choice of 20 m, rather than the more commonly used 10-meter depth, was intentional because the input bathymetry used in this study has a resolution of 500 m, making the coastline detail less refined. Setting up the gauge stations at the 10-meter depth would cause issues in areas like Port of Manila, where the 10-meter depth contour is in close proximity to the coastline. To ensure more conservative and stable results, we placed the gauges at the 20-meter depth.

Modelling results and discussions

A magnitude 8.8 earthquake originating from the southern Manila Trench would generate multiple tsunamis propagating toward Manila Bay. At the instant of the earthquake (time = 0), the virtual gauge at 100 m depth near the bay entrance recorded a 5 m wave height (labelled '1' in Fig. 4a). The wave then subsides, reaching a minimum of −0.9 m at the 20-minute mark, before rising above mean sea level (msl) at 27 min. This second positive wave peaks at 0.9 m at 31 min (labelled '2' in Fig. 4a). The wave subsequently drops below msl for the next hour, before rising again at the 1.8-hour mark. This third wave reaches a peak of 1 m at 2.05 h (labelled '3' in Fig. 4a). Wave activity at the bay entrance continues to fluctuate over the remaining hours of the simulation; however, the maximum heights only reach approximately 0.6 m, occurring at the 4.1-hour and 9.7-hours marks.

By examining the tsunami simulation snapshots (Fig. 4b-d), we identified the mechanisms responsible for the formation of three distinct wave series within the first two hours. The snapshots also highlight two key roles played by the submarine canyon-located along the continental slope that separates the deeper waters from the shallower continental shelf-in the propagation of tsunami waves. For tsunamis originating in deeper waters, the canyon acts as a funnel, channelling and accelerating wave energy toward the bay, as its shallow tip is pointed directly toward the bay entrance. In contrast, for tsunamis already in the continental shelf, the canyon restricts wave propagation toward the open sea and instead redirects the waves into Manila Bay. The animation showing the simulation snapshots is provided in the Supplemental Data section of this paper (Felix 2025).

The first wave at t = 0 is generated by the instantaneous seafloor uplift during the earthquake. Its propagation show how the submarine canyon funnels the wave toward the bay. The tsunami wave front conforms to the shape of the canyon's tip, as shown in the simulation snapshot at 20 min (Fig. 4b), where the colour gradient of the high wave curves concavely around the pointed tip of the canyon. This behaviour is consistent with the findings of Iglesias et al (2014), based on simulations of

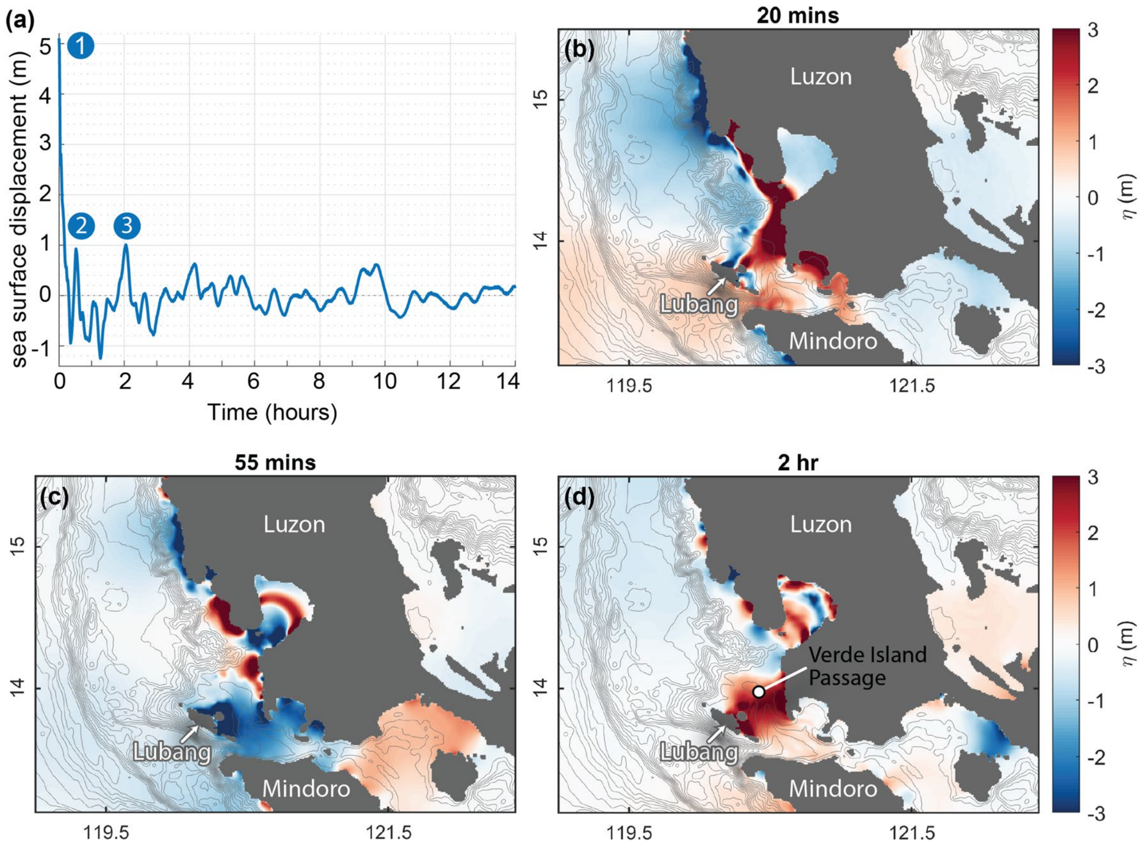

Fig. 4 (**a**) Tsunami waveform recorded at the virtual gauge station at the mouth of Manila Bay. (**b-d**) Snapshots of sea surface displacement at 20 min, 55 min, and 2 h after the earthquake

hypothetical tsunami scenarios using synthetic bathymetry, as well as real bathymetric data from the Blanes Canyon in the Western Mediterranean Sea.

The second series of waves entering the bay results from a combination of reflected and refracted waves along the shallow western coast of Luzon Island-particularly at the headlands of Manila Bay-along with waves funneled through the canyon from deeper waters (Fig. 4c).

The third series of high waves primarily originates from refracted and reflected waves in the southwestern region-between Luzon, Mindoro, and Lubang Islands-which propagate through the Verde Island Passage. The nearly east–west strike of the canyon, combined with the northwest orientation of the elongated Lubang Island, forms an almost L-shaped barrier that restricts shallow-water pathways. This configuration redirects tsunamis travelling through the Verde Island Passage toward Manila Bay, rather than allowing them to disperse into the South China Sea (Fig. 4d).

We analysed how these multiple propagated waves are recorded by nearshore gauge stations located at a depth of 20 m: at the northern headland (Bataan Station), the southeastern coast within the bay (Cavite Station), and Port of Manila in the inner eastern section (Fig. 5). All gauge records at this depth indicate that the earthquake

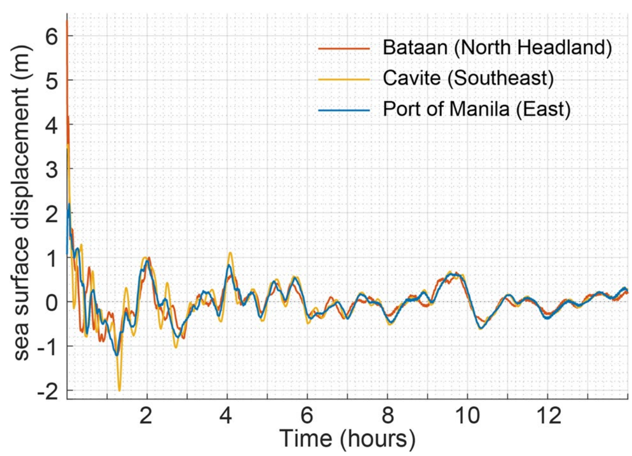

Fig. 5 Gauge records at 20 m water depth over the 14-hour simulation. The highest waves occurred almost instantaneously with the earthquake. Multiple waves following the initial peak are recorded throughout the simulation

rupture caused an instantaneous, or nearly instantaneous, sea surface uplift. In addition, multiple waves continued to be recorded for several hours following the earthquake. In all three gauge records, the first wave was the highest observed during the entire simulation, with recorded heights of 6.3 m, 3.8 m, and 2.8 m for Bataan, Cavite, and Port of Manila, respectively.

Assuming a 1 m threshold for relevant tsunamis, other notable arrival times include the 19-minute mark, the 2-hour mark, and the 4-hour-and-5-minute mark (Fig. 5). For the gauges within the bay (Cavite and Port of Manila), the second-highest peak occurred at the 19-minute mark, with wave heights of 1.3 m at Cavite and 2.2 m at Port of Manila. At the 2-hour mark, all three stations recorded peak heights ranging from 1.0 to 1.2 m. At the 4-hour-and-5-minute mark, Cavite and Port of Manila again recorded peak heights between 1.1 and 1.2 m. These gauge records support the earlier analysis, indicating that multiple waves propagated into Manila Bay and contributed to sustained wave amplification within the bay.

The maximum wave height map shows that the highest impacts are concentrated at the bay's entrance headlands and along the northeast-striking southern coast of Manila Bay, within the provinces of Bataan and Cavite (Fig. 6). While these areas experience the highest wave heights, other parts of the Manila Bay coastline are also exposed to elevated wave conditions. In addition to the incoming waves from outside the bay, the high wave amplitudes observed within Manila Bay can be attributed to constructive interference between reflected and refracted waves trapped inside the bay. Although destructive interference may also occur, reducing wave energy in certain areas, the overall results suggest that constructive interference dominates, leading to consistently high wave heights throughout the bay. In terms of maximum current velocity, the entire coastline of Manila Bay is exposed to extremely high values. According to the study by Lynett et al (2014), the current velocities observed in this study fall within the range capable of causing extreme damage to maritime assets.

The maximum wave height maps presented in this paper should be interpreted as minimum estimates of the expected maximum wave height, given that we used a coarse-resolution grid in our modelling. Using a finer grid resolution in the modelling would likely result in higher wave height estimates. This interpretation is based on a previous study, which showed that using a coarse-resolution grid substantially underestimates maximum wave heights compared to models with 10–50 m resolution Felix et al (2024). Regarding wave arrival time, the results presented in this paper should be treated as rough estimates. Felix et al (2024) have shown no consistent trend in arrival times when comparing models using coarse and fine grid resolutions. Therefore, whilst the timing may not be definitive, the results still provide a general indication of the wave arrival times.

Preliminary assessments of tsunami hazards are often conducted using coarse-resolution grids (e.g., Heidarzadeh et al 2025; Tsukanova et al 2025; Verolino et al 2025a). In this study, we have adopted a similar approach, using a coarse resolution of 500 m. Whilst such a resolution may not capture nearshore dynamics as accurately as models with finer grids in shallow areas (Felix et al 2024), our findings remain relevant. This is because the large-scale features (Corregidor Island, Lubang Island, and the submarine canyon) that are key

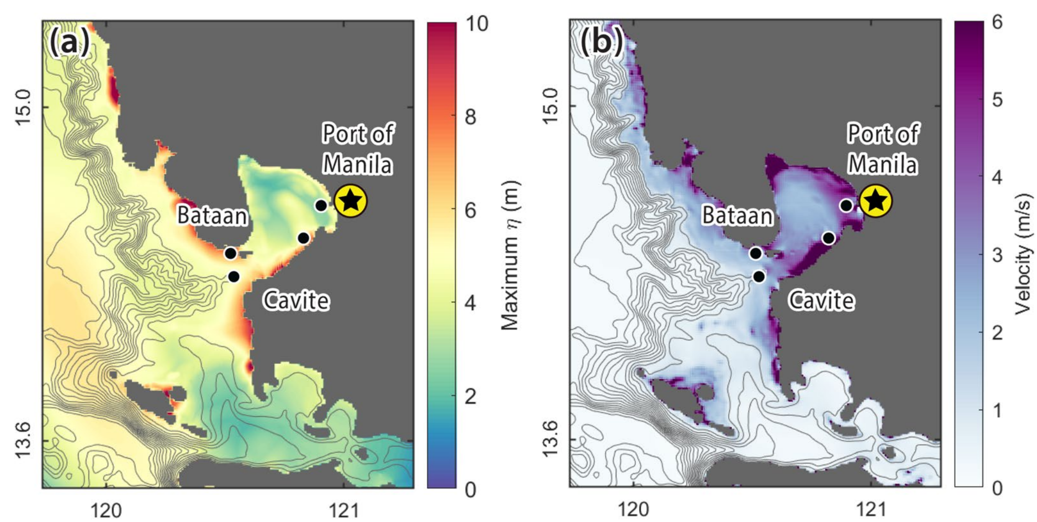

Fig. 6 Maps of (**a**) maximum wave height and (**b**) maximum current velocities in Manila Bay over a 14-hour simulation period. The provinces of Bataan and Cavite experience the highest wave heights and current velocities. Dots - gauge stations

factors influencing tsunami behaviour in this region are well represented at this resolution. Corregidor Island, located at the centre of the mouth of Manila Bay, has dimensions approximately 1 to 4 times larger than the 500-meter grid size. Lubang Island and its neighbouring smaller islands, situated southwest of the Manila Bay, range from 8 to 20 times larger than the grid resolution. The submarine canyon outside the bay is even more prominent, with dimensions roughly 60 to 120 times larger than the grid size. These proportions confirm that the coarse grid is sufficient to capture the main features influencing the tsunami behaviour in our study area.

Although the main feature of FUNWAVE-TVD is its implementation of the Boussinesq equations, we opted to use its linear shallow water equation function in this study as it is sufficient to demonstrate the general tsunami impact in the region. Adopting the use of a Boussinesq-type model in combination with a coarse grid resolution may introduce unnecessary noise in the simulated wave peaks, as the model attempts to resolve dispersive effects that are not significant at this scale or aligned with the goals of this study. Overall, the findings of this study provide a useful basis for identifying specific regions within Manila Bay where nested, higher-resolution grids could be applied in future work to support more detailed tsunami impact assessments.

The main takeaway from this initial assessment of tsunami hazard in Manila Bay is that the highest wave occurs almost instantaneously during the earthquake. In the scenario presented in this study, tsunami warnings for communities around Manila Bay should remain active even after the initial and largest wave has passed, and should be maintained for at least two hours. This is due to the continued arrival of subsequent waves. Although smaller, these subsequent waves still pose a hazard, particularly when combined with wave interference effects occurring within the bay. Throughout the entire simulation duration, we showed that the most impacted areas are the headlands of the bay and, within the bay itself, the southeastern coastline.

Additional work is needed to better quantify the tsunami hazard in Manila Bay resulting from a rupture of the southern segment of the Manila Trench. The analyses presented in this study have not previously been conducted in this region with this level of detail. Our work identifies the key factors influencing tsunami behaviour in the bay and highlights the locations most affected, representing a step forward in understanding the hazard. We hope that this study will support and encourage further in-depth research into the tsunami hazard in Manila Bay and its potential impact on communities along the coastline.

Conclusions

We developed free, offline standalone applications by leveraging the open-source nature of the FUNWAVE-TVD model and successfully applied them in a preliminary assessment of tsunami hazard in Manila Bay. These apps bridge the gap between the tsunami model and researchers by simplifying the learning process and making the tool accessible to a broader, multidisciplinary audience. They enhance workflow efficiency and reduce the time required for model setup, allowing researchers to focus more on post-modelling tasks such as data analysis and manuscript preparation.

Supplementary Information

The online version contains supplementary material available at https://doi.org/10.1186/s40562-025-00422-5.

Supplementary material 1

Supplementary material 2

Acknowledgements

This research is supported by the Earth Observatory of Singapore via its funding from the National Research Foundation Singapore and the Singapore Ministry of Education under the Research Centres of Excellence initiative. This work comprises EOS contribution number 632. We extend our gratitude to Edwin Tan Seng Tat for his valuable assistance in supporting us on utilising the High Performance Computing at Nanyang Technological University High Performance Computing Centre (NTU HPC). Thanks to his support, we were able to conduct the tsunami simulations using the HPC. The authors gratefully acknowledge Nick McCullen from the Department of Architecture and Civil Engineering, and Roberto Scipioni from the Research Computing Group at the University of Bath (doi.org/10.15125/b6cd-s854), for their support and guidance in using the University of Bath's HPC.

Author contributions

RF: Conceptualisation, Modelling, Software, Visualization, Formal analysis, Writing – original draft. ETHZ: Writing – original draft (Manila Trench tectonic setting and tsunami source setup), Modelling, Writing – review & editing, Software validation. MW: Writing – original draft (FUNWAVE-TVD description), Writing – review & editing, Software validation. AV: Writing – review & editing, Software validation. PJY: Writing – review & editing, Software validation. AS: Conceptualisation, Writing – review & editing; Supervision; Funding acquisition.

Funding

This research is supported by the Earth Observatory of Singapore via its funding from the National Research Foundation Singapore and the Singapore Ministry of Education under the Research Centres of Excellence initiative. This work comprises EOS contribution number 632. Raquel Felix acknowledges that the final stages of this work were completed with the support of the United Kingdom Research and Innovation (UKRI) grant EP/Z001080/1.

Data availability

No datasets were generated or analysed during the current study.

Code availability

The FUNMAP apps, user manuals, and the source codes are available for download at this link: https://github.com/raquelpfelix.

Material availability

Not Applicable

Declarations

Ethics approval and consent to participate
Not applicable.

Consent for publication
All the authors read and approved the publication of this work.

Competing interests
The authors declare no Competing interests

Received: 30 June 2025 Accepted: 22 September 2025
Published online: 16 October 2025

References
Armada LT, Hsu SK, Dimalanta CB et al (2020) Forearc structures and deformation along the manila trench. Journal of Asian Earth Sciences X 4:100036
Bautista BC, Bautista MLP, Oike K et al (2001) A new insight on the geometry of subducting slabs in northern luzon, philippines. Tectonophysics 339:279–310
Blaser L, Krüger F, Ohrnberger M et al (2010) Scaling relations of earthquake source parameter estimates with special focus on subduction environment. Bull Seismol Soc Am 100(6):2914–2926
Felix R (2025) Supplementary materials for "FUNWAVE-based Open-Access Mapping Applications (FUNMAP) Applied to Tsunami Modelling from the Manila Trench to Manila Bay, Philippines". https://doi.org/10.15125/BATH-01553, Bath: University of Bath Research Data Archive
Felix R, Hubbard J, Wilson K et al (2024) Heatmap analysis of modeled coastal tsunamis using different bathymetry data resolutions. Geoscience Letters 11(1):1–13
GEBCO Compilation Group (2024) GEBCO 2024 Grid. https://doi.org/10.5285/1c44ce99-0a0d-5f4f-e063-7086abc0ea0f
Glimsdal S, Pedersen GK, Harbitz CB et al (2013) Dispersion of tsunamis: does it really matter? Nat Hazard 13(6):1507–1526, https://doi.org/10.5194/nhess-13-1507-2013, https://nhess.copernicus.org/articles/13/1507/2013/
Heidarzadeh M, Gusman AR, Mulia IE, et al (2025) Tsunami hazards and risks from the philippine trench: The cases of 2012 and 2023 mw 7.6 tsunamigenic earthquakes. Ocean Engineering 329:120985
Hsu YJ, Yu SB, Song TRA et al (2012) Plate coupling along the manila subduction zone between taiwan and northern luzon. J Asian Earth Sci 51:98–108
Hsu YJ, Yu SB, Loveless JP et al (2016) Interseismic deformation and moment deficit along the manila subduction zone and the philippine fault system. Journal of Geophysical Research Solid Earth 121(10):7639–7665
Iglesias O, Lastras G, Souto C et al (2014) Effects of coastal submarine canyons on tsunami propagation and impact. Mar Geol 350:39–51
Keiiti A (1966) Generation and propagation of g waves from the niigata earthquake of june 16, 1964: part 1. a statistical analysis. Bulletin of the Earthquake Research Institute University of Tokyo 44:23–72
Kirby JT, Wei G, Chen Q, et al (1998) FUNWAVE 1.0: Fully Nonlinear Boussinesq Wave Model - Documentation and User's Msanual. Tech. rep., University of Delaware
Lesser GR, Jv R, van Kester JTM et al (2004) Development and validation of a three-dimensional morphological model. Coast Eng 51(8–9):883–915
Li L, Switzer AD, Chan CH et al (2016) How heterogeneous coseismic slip affects regional probabilistic tsunami hazard assessment: a case study in the south china sea. Journal of Geophysical Research Solid Earth 121(8):6250–6272
Liang D, Liu H, Tang H et al (2013) Comparison between boussinesq and shallow-water models in predicting solitary wave runup on plane beaches. Coast Eng J 55(04):1350014
Lin P, Liu PLF (1998) A numerical study of breaking waves in the surf zone. J Fluid Mech 359:239–264
Lin SC, Wu TR, Yen E et al (2015) Development of a tsunami early warning system for the south china sea. Ocean Eng 100:1–18
Linthon M, Koshimura S (2019) Study of the bathymetric influence on tsunami propagation near the coast of Esmeraldas by tsunami simulation and ray tracing analysis. Synopsis of iisee-grips master's thesis, International Institute of Seismology and Earthquake Engineering
Lu CH, Yen JY, Chyi SJ et al (2019) Geological records of south china sea tsunamis on penghu islands. Taiwan Journal of Asian Earth Sciences 177:263–274
Lynett PJ, Borrero J, Son S et al (2014) Assessment of the tsunami-induced current hazard. Geophys Res Lett 41(6):2048–2055
Mai PM, Beroza GC (2002) A spatial random field model to characterize complexity in earthquake slip. Journal of Geophysical Research: Solid Earth 107(B11):ESE–10
Mai PM, Beroza GC (2000) Source scaling properties from finite-fault-rupture models. Bull Seismol Soc Am 90(3):604–615
Megawati K, Shaw F, Sieh K, et al (2009) Tsunami hazard from the subduction megathrust of the south china sea: Part i. source characterization and the resulting tsunami. Journal of Asian Earth Sciences 36(1):13–20
Merati N, Chamberlin C, Moore C, et al (2010) Integration of tsunami analysis tools into a GIS workspace–research, modeling, and hazard mitigation efforts within NOAA's Center for Tsunami Research. Geospatial Techniques in Urban Hazard and Disaster Analysis pp 273–294
Nguyen PH, Bui QC, Vu PH et al (2014) Scenario-based tsunami hazard assessment for the coast of vietnam from the manila trench source. Phys Earth Planet Inter 236:95–108
Okada Y (1985) Surface deformation due to shear and tensile faults in a half-space. Bull Seismol Soc Am 75(4):1135–1154
Papazachos B, Scordilis E, Panagiotopoulos D et al (2004) Global relations between seismic fault parameters and moment magnitude of earthquakes. Bulletin of the Geological Society of Greece 36(3):1482–1489
PHIVOLCS (2024) Briefer on the Magnitude (Mw) 5. Offshore Ilocos Norte Earthquake as of 31 December 2024. Tech. rep., Philippine Institute of Volcanology and Seismology
Qiu Q, Li L, Hsu YJ et al (2019) Revised earthquake sources along manila trench for tsunami hazard assessment in the south china sea. Nat Hazard 19(7):1565–1583
Ramos NT, Tsutsumi H, Perez JS et al (2012) Uplifted marine terraces in davao oriental province, mindanao island, philippines and their implications for large prehistoric offshore earthquakes along the philippine trench. J Asian Earth Sci 45:114–125
Roelvink D, Reniers A, Van Dongeren A et al (2009) Modelling storm impacts on beaches, dunes and barrier islands. Coast Eng 56(11–12):1133–1152
Roelvink D, McCall R, Mehvar S et al (2018) Improving predictions of swash dynamics in xbeach: the role of groupiness and incident-band runup. Coast Eng 134:103–123
Shi F, Kirby JT, Harris JC et al (2012) A high-order adaptive time-stepping tvd solver for boussinesq modeling of breaking waves and coastal inundation. Ocean Model 43:36–51
Sun L, Zhou X, Huang W et al (2013) Preliminary evidence for a 1000-year-old tsunami in the south china sea. Sci Rep 3(1):1655
Sun Z, Niu X (2025) Quantifying probabilistic tsunami inundation risk and its application to the Guangdong-Hong Kong-Macao Greater Bay Area. International Journal of Disaster Risk Reduction p 105217
Tan E, Li L, Qiu Q, et al (2023) A Stochastic Model of Potential Tsunami Impacts Originating from the Southern Part of the Manila Trench. In: AOGS General Assembly Conference Abstracts
Tolman HL, et al (2009) User manual and system documentation of WAVEWATCH III TM version 3.14. Technical Note, MMAB Contribution 276(220)
Tsukanova E, Medvedev I, Heidarzadeh M et al (2025) Tsunami propagation from the 2024 noto peninsula earthquake across the sea of japan: observations and modelling. Ocean Eng 336:12173, https://doi.org/10.1016/j.oceaneng.2025.121730, https://www.sciencedirect.com/science/article/pii/S0029801825014362
USGS (2024) Earthquake Catalogue Search. https://earthquake.usgs.gov/earthquakes/search/, Earthquake Hazards Program, United States Geological Survey
Van Ormondt M, Nederhoff K, van Dongeren A (2020) Delft dashboard: a quick set-up tool for hydrodynamic models. J Hydroinf 22(3):510–527
Verolino A, Watanabe M, Felix R, et al (2025a) An initial assessment of volcanic meteo-tsunami hazard in the south china sea: what we learned and how to move forward. Georisk: Assessment and Management of Risk for Engineered Systems and Geohazards pp 1–21

Verolino A, Watanabe M, Felix R, et al (2025b) Forced and free waves of simulated volcanic meteo-tsunamis in the South China Sea. npj Natural Hazards 2(1):25
Wang X, Power W, Staff G (2011) COMCOT: a tsunami generation propagation and run-up model. GNS Science, Science Report, p 43
Watanabe M, Arikawa T, Kihara N et al (2022) Validation of tsunami numerical simulation models for an idealized coastal industrial site. Coast Eng J 64(2):302–343
Wei G, Kirby JT, Grilli ST et al (1995) A fully nonlinear boussinesq model for surface waves. part 1. highly nonlinear unsteady waves. J Fluid Mech 294:71–92
WorldPop (2024) Philippines - Spatial Distribution of Population (2015-2030). https://data.humdata.org/dataset/worldpop-population-counts-2015-2030-phl, constrained population estimates at 100m resolution, updated annually. Accessed June 20, 2025
Wu TR (2012) Deterministic study on the potential large tsunami hazard in taiwan. Journal of Earthquake and Tsunami 6(03):1250034
Wu TR, Huang HC (2009) Modeling tsunami hazards from manila trench to taiwan. J Asian Earth Sci 36(1):21–28
Yu KF, Zhao JX, Shi Q et al (2009) Reconstruction of storm/tsunami records over the last 4000 years using transported coral blocks and lagoon sediments in the southern south china sea. Quatern Int 195(1–2):128–137

Publisher's Note